Experimental Investigation of Natural Convection Heat Loss From a Model Solar Concentrator Cavity Receiver

T. Taumoefolau
e-mail: tuifua.taumoefolau@anu.edu.au

S. Paitoonsurikarn

Centre for Sustainable Energy Systems,
Department of Engineering,
Australian National University,
Canberra ACT 0200,
Australia

G. Hughes
Research School of Earth Sciences,
Australian National University,
Canberra ACT 0200,
Australia

K. Lovegrove
Centre for Sustainable Energy Systems,
Department of Engineering,
Australian National University,
Canberra ACT 0200,
Australia

Natural convection heat loss inevitably occurs in cavity-type receivers in high concentrating solar dishes, downward focusing systems and solar towers. In most applications, it can contribute a significant fraction of total energy loss, and hence it is an important determining factor in system performance. To investigate natural convection losses from cavity type receivers, an electrically heated model receiver, was tested at inclinations varying from −90 deg (cavity facing up) to 90 deg (cavity facing straight down), with test temperatures ranging from 450 to 650 deg C. Ratios of the aperture diameter to cavity diameter of 0.5, 0.6, 0.75, 0.85 and 1.0, were used. In addition to measurements of overall heat loss, the Synthetic Schlieren technique was used to visualize the flow pattern out of the cavity. Numerical modeling of the convection losses from the cavity was carried out for positive angles with the commercial computational fluid dynamics software package, Fluent 6.0. Good agreement was found between the numerical flow patterns at the aperture region with the schlieren images and between measured and predicted values for heat loss. Of the previously published work that has been reviewed, a model proposed by Clausing, A. M., 1981, "An Analysis of Convective Losses from Cavity Solar Central Receivers," Sol. Energy ***27*** *(4) pp. 295–300 shows the closest prediction to both numerical and experimental results for downward facing cavities despite its original use for bigger-scale central receivers.* [DOI: 10.1115/1.1687403]

Keywords: *Natural Convection, Solar Cavity Receiver, Dish Concentrator*

1 Introduction

In solar energy thermal systems, heat loss mechanisms can significantly reduce the efficiency and consequently the cost effectiveness. It is therefore vital to fully understand the nature of these heat loss mechanisms. With paraboloidal dish cavity receivers, conduction and radiation can readily be determined analytically, however the complexity of the geometry, temperature and velocity fields, in and around the cavity makes it considerably harder to determine the convection loss.

The Australian National University (ANU) has been involved with the investigation of solar thermal energy conversion using paraboloidal dish concentrators for many years. Currently the team is working with a 400 m^2 concentrator fitted with a monotube boiler, cavity receiver for superheated steam production and a 20 m^2 concentrator that operates a cavity receiver lined with reactor tubes for ammonia dissociation for energy storage [2].

This paper reports on investigation of the convection losses from a small, electrically heated, laboratory simulation of a solar cavity receiver, which has been constructed to measure losses directly. Flow visualization using the Synthetic Schleiren technique has also been employed. The results from this system have then been used in comparison with the predictions obtained from a range of published models plus calculations with Computational Fluid Dynamics (CFD) using the ''Fluent 6.0'' software package.

1.1 Previous Work. There have been several previous investigations of convection losses from cavity receivers. An analytical model of large cubical central receivers was proposed by Clausing [1], based on the local convective heat transfer coefficients inside the cavity, determined from standard semi-empirical correlations and the energy transferred by the air through the aperture due to buoyancy and wind effects. This model was later refined and verified by the same author [3], with experimental results from a 2.7 m square aperture receiver and good agreement found.

Clausing [4] conducted an experimental study on a 0.4 m cubic cavity with a variety of side facing apertures. A cryogenic wind tunnel was used with temperatures ranging from −193 to 37 deg C in order to reduce the effect of radiative heat transfer. Thin foil heaters were used to heat each cavity side and the convective loss was deduced from the cooling rate of each side after the heaters were turned off. This study resulted in further development of the Clausing [3] model to include the effect of aperture area. The improved model showed good agreement with the experimental data.

Harris [5] described an experimental study by Koenig & Marvin [6], which developed a correlation that explicitly includes parameters such as inclination angle and aperture size.

Stine & McDonald [7] proposed a correlation based on experimental results from a single tube cylindrical-frustum shaped receiver. The receiver had a length of 914 mm, an outer diameter of 813 mm and an aperture diameter of 457 mm. Tests were carried out with receiver inclinations between 0 and 90 deg with ''Syltherm 800'' heat transfer fluid pumped through the receiver to create test temperatures of up to 315 deg C. The total heat loss was determined from the temperature drop of the heat transfer fluid across the receiver.

Leibfried [8] carried out experimental studies that simulated operation in both downward focusing systems and paraboloidal dish systems. This study used electrically heated spherical and hemispherical receivers with a diameter of 400 mm. The aperture for these receivers ranged from 60 to 195 mm in diameter and was adjusted by adding insulated disks of different inner diameters.

Contributed by the Solar Energy Division of THE AMERICAN SOCIETY OF MECHANICAL ENGINEERS for publication in the ASME JOURNAL OF SOLAR ENERGY ENGINEERING. Manuscript received by the ASME Solar Energy Division, August, 2003; final revision, December 2003. Associate Editor: A. Kribus.

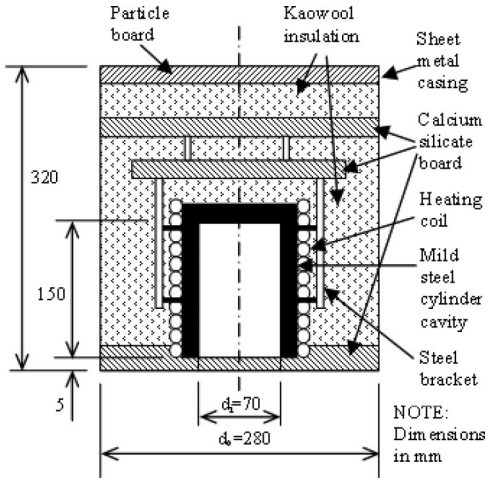

Fig. 1 Cross section sketch of model receiver

They modified Clausing's [4] and Stine & McDonald's [7] models to account for the different flow pattern while the cavity is facing upwards. The two modified correlations were in good agreement with their experimental results. The Rayleigh number (Ra) in the experiments was estimated to be between 10^7 and 10^9, indicating that the flow regime within most of the boundary layer would be laminar.

With all these studies the range of applicability beyond the receiver geometry directly examined remains unclear and therefore caution should be used when using them for different geometries and operating conditions.

2 Laboratory Measurement of Convection Losses

2.1 Experimental Apparatus. An electrically heated experimental simulation of a cavity receiver has been constructed to allow direct measurement of losses under laboratory conditions. The details of the model receiver are shown in Fig. 1 and the arrangement in the laboratory in Fig. 2. The model receiver consists of a mild steel tube cavity with a ''Pyrontenax'' mineral insulated electrical heater cable wound around it as a source of heat input. The cavity interior surface has been painted with high temperature resistant black ''Pyromark'' 2500 paint. The steel tube is mounted in a framework of Calcium Silicate insulation board. The entire structure is covered by a sheet metal casing and all internal spaces filled with ''Kaowool'' ceramic insulation material.

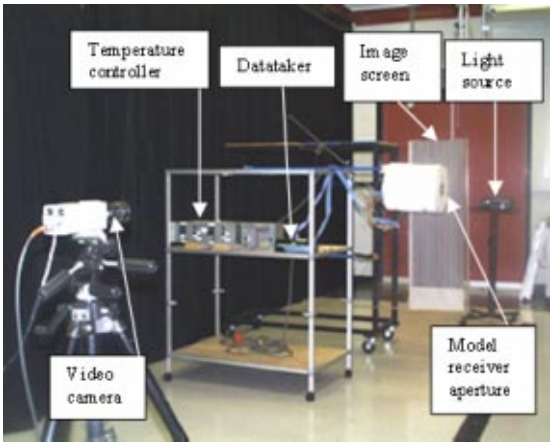

Fig. 2 Experimental setup

The size of the aperture was altered by placing 5 mm thick calcium silicate washers with inner diameters ranging from 35 to 59.5 mm.

The model receiver is attached to the left of a trolley by a hinged angle adjustment mechanism to enable testing at different angles. There are 7 K-type thermocouples that measure the cavity surface temperature, 8 on the exterior surface of the model, plus a further 8 measuring various temperatures within the model. These thermocouples are logged with a Datataker 600. The temperature of the cavity is controlled by a self tuned Eurotherm 808 PID temperature controller that regulates the power level to the heating coil. A host computer, not shown in Fig. 2, acquires both the data from the temperature controller and the Datataker.

During operation, a time interval of approximately one hour is required for the system to reach steady state. Temperatures are logged at 15 second intervals and the power level is logged at four second intervals for a period of 20 minutes, to provide the data for a reliable steady state data point. A ''Fluke 83'' multimeter was used to measure the supply voltage (V), and heater resistance (R). These values in conjunction with the regulated power level (p_L), were used to determine the total heat loss rate (q_t) from the receiver using Eq. (1):

$$q_i = p_L \frac{V^2}{R}. \tag{1}$$

2.1.1 Flow Visualization. The convective flow outside the cavity receiver was visualized using the 'Synthetic Schlieren' technique [9]. Schlieren techniques rely on the deflection of light rays passing through an optical medium in response to gradients in the refractive index field normal to the ray direction. The ray deflection increases with refractive index gradient, thus observation of the deflection field reveals detail of the refractive index (density) structure in the medium.

In this study, the refractive index field is a function of temperature in the convective flow. The model receiver was positioned between a video camera (Cohu 4910 Series High Performance monochrome CCD) and a back-illuminated image screen, as shown in Fig. 2. The image screen consisted of a series of fine parallel lines aligned normal to the axis of the cavity receiver, so as to detect temperature gradients in the direction of the cavity axis. Maximum sensitivity was achieved by aligning the lines of the camera CCD with the lines of the image screen. Thermal structures in the convective flow distort the pattern of parallel lines recorded by the camera, and these structures become evident upon comparing the distorted pattern with a reference pattern captured prior to heating the cavity. The comparison (a pixel-by-pixel based subtraction) was carried out using a PC, a frame-grabber (Data Translation DT2862) and the flow imaging software, ''DigImage'' [10].

2.2 Determination of the Energy Balance. The experimental arrangement provides a direct measurement of overall thermal losses from the cavity. Since it is convection loss (q_{conv}) that is of interest, conduction (q_{cond}) and radiation (q_{rad}) contributions need to be accounted for in the energy balance, according to Eq. (2):

$$q_{conv} = q_t - q_{cond} - q_{rad}. \tag{2}$$

2.2.1 Conduction Loss Measurement. To determine the conduction heat loss, measurements of loss were made with the cavity inverted and with an insulated plug in the aperture. The internal and external temperatures of the plug were measured and used to determine the plug conduction loss. Heat loss through the insulated case will be determined by the thermal resistance of the insulation material and the natural convection process on the outer surface acting in series. The thermal resistance due to natural convection would in principle be angle dependant however it is much

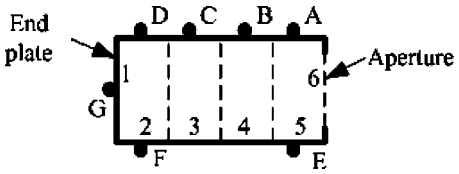

Fig. 3 Cavity division for radiation calculation and thermocouple location

smaller than the resistance due to the insulation material. It is therefore assumed that conduction is the same for all inclination angles.

Finite Element analysis of the conduction problem using STRAND 7 release 1.03 has also been carried out. Agreement to within 10% was found and the difference attributed to the uncertainty in the actual effective conductivity of the insulation material.

2.2.2 Radiation Loss Calculation. Radiation loss has been determined analytically with the network method described by Holman [11], where the surface is assumed to be gray and radiation is uniformly diffuse. Figure 3 shows the cavity divided into 6 sections and location of thermocouples A-G, measuring the cavity surface temperature, which is used to determine the net radiation from each section.

The radiation energy balance for a section is given by Eq. (3);

$$J_i = \frac{1}{1 - F_{ii}(1-\varepsilon_i)} \left((1-\varepsilon_i) \sum_{j \neq i} F_{ij} J_j + \varepsilon_i E_{b_i} \right) \tag{3}$$

where J_i is the radiosity, F_{ij} is the fraction of radiant energy leaving surface i and reaching surface j, ε_i is the surface emissivity and E_{bi} is the black body emissive power.

Having set up an equation for each surface, the set of 6 equations is then solved simultaneously to calculate the radiosities. The net radiation transfer rate for a surface i is given by Eq. (4):

$$q_i = \frac{\varepsilon_i A_i}{1-\varepsilon_i} (E_{b_i} - J_i) \tag{4}$$

where A_i is the area of the surface. The radiation loss through the aperture is then obtained from the sum of individual radiation losses.

Emissivity for the "Pyromark" painted cavity surface was obtained from McDonald [12]. It ranges from 0.87 for a cavity temperature of 450 deg C to 0.88 for a cavity temperature of 650 deg C. With the high emissivity of the paint, the uncertainty in the radiation loss calculation is mainly due to the uncertainty in the experimental temperature measurements.

3 Numerical Analysis

The CFD Software Package, Fluent 6.0 [13] was employed in the 3D simulation of the natural convection through the aperture of the cavity receiver.

3.1 Problem Formulation. Figure 4 schematically represents the formulated flow configuration. In reality, the receiver is surrounded by an infinite atmosphere with a limiting temperature equal to ambient air temperature. In the CFD analysis, this needs to be approximated by placing the receiver in a sufficiently large enclosure with walls at ambient temperature. The geometry of this arrangement is illustrated in Fig. 4. Note that, due to the symmetrical flow geometry with respect to the middle vertical plane, the computational extent comprises only one half of the physical domain shown in Fig. 4.

The size of the enclosure was increased until it had an insignificant effect on fluid and heat flows in the vicinity of the receiver. It was found that the diameter of the cylindrical enclosure should be about twenty times the diameter of the receiver to achieve this.

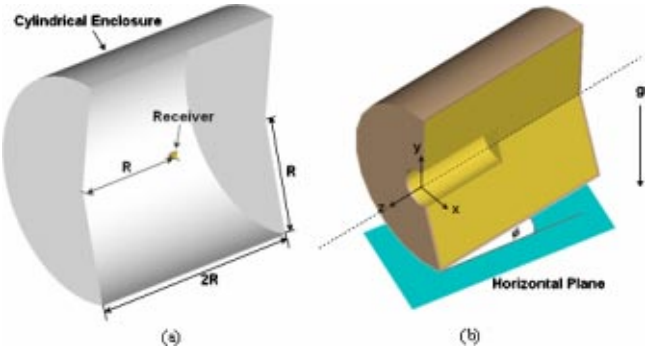

Fig. 4 Schematic diagram of flow configuration: (*a*) receiver location in the domain, (*b*) receiver close up

Grid dependency was investigated and the final grids used consist of approximately 2×10^5 hexahedral cells. The cells are very small in the region inside the cavity and nearby the receiver but increase in size gradually toward the cylindrical enclosure wall. Figure 5 shows the grid pattern used.

3.2 Modeling Equations. The flow and heat transfer simulation is based on the simultaneous solution of the system of equations describing the conservation of mass, momentum, energy and turbulent transport property. The Spalart-Allmaras one-equation turbulent model recommended by Spalart [14] is employed.

The steady-state governing equations are solved in Fluent using a coupled solver, which means that temperature and flow fields are coupled with each other and are solved simultaneously. All temperature-dependent properties of air are evaluated at local temperature by using the least-square fit equations derived from thermodynamic data compilations taken from Holman [11].

3.3 Boundary Conditions. An isothermal boundary condition was applied to the cavity wall, whereas the outer walls of the receivers were assumed to be adiabatic. The cavity wall temperatures used were the average experimental temperatures for the cylindrical section and the end plate.

The wall temperature of the entire cylindrical enclosure was set to an ambient temperature of 27 deg C. Normal velocity and normal gradients of all flow variables were set to zero across the vertical plane of symmetry. The inclination of the cavity as shown in Fig. 4(*b*) was simulated by redirecting the gravity vector to the desired direction. The gravitational constant was specified to the standard value of 9.80665 m/s^2.

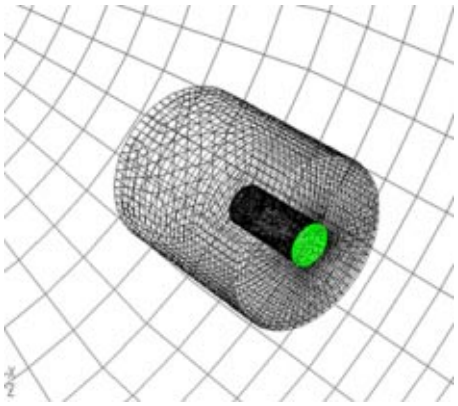

Fig. 5 Typical computational grid

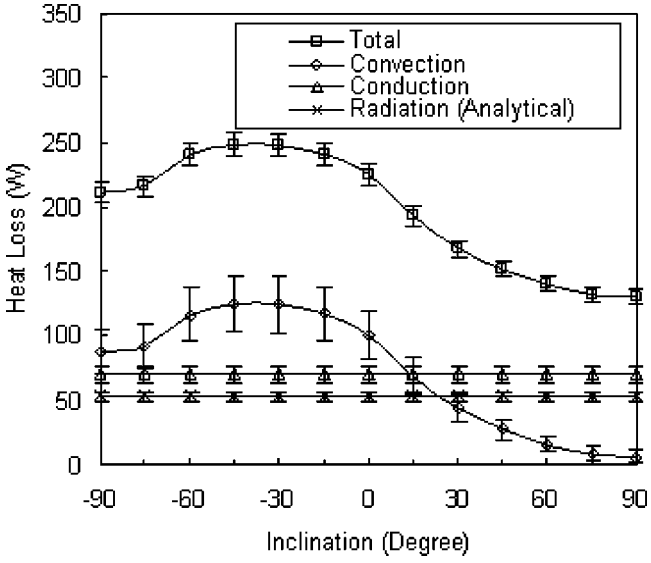

Fig. 6 Experimental heat loss with Tc=445 deg C and fully open cavity

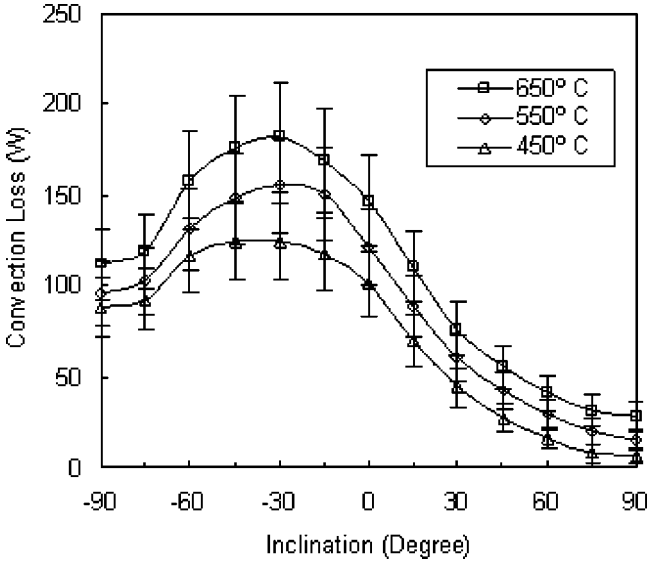

Fig. 7 Convection heat loss from a fully open cavity

4 Results and Discussions

4.1 Experimental Results. Figure 6 presents the results of heat loss measurements for the model receiver operating at a set point temperature of 450 deg C. The average experimental cavity temperatures (T_c) were 445 deg C for the cylindrical section and 420 deg C for the end plate. At 90 deg inclination the variation in temperature from the front (aperture) to the back of the cavity is 10 deg C and at 0 deg inclination the variation between the top to the bottom of the cavity is 20 deg C. Radiation losses were calculated to be constant at 53.4 ± 3.1 W and the effect of variation in temperature within the cavity due to inclination is within the uncertainty of ± 3.1 W. Conduction losses were measured to be constant at 70.4 ± 6.1 W and measurements of overall ''conduction loss'' were made over a range of angles and no angle dependence could be resolved within the error bars of the measurements. The maximum convection loss occurs at -45 deg when it represents 50.1% of the total heat loss. As is expected, the minimum convection loss occurs when the receiver is pointing vertically downward (90 deg inclination), and comprises 4.8% of the total heat loss. In this orientation, the high temperature buoyant air remains stagnant within the cavity. As the receiver inclination is reduced from -45 deg to -90 deg (facing vertically upward), the convection loss also reduces which is mainly due to the impediment of the outflow from the cavity by the inflow.

Convection loss for three cavity temperatures is compared in Fig. 7. They all show a similar dependence on inclination as that described for the convection loss in Fig. 6. It is also evident that the losses increase with higher cavity temperatures throughout all inclinations as expected. It is worth noting, that the convection losses although at a minimum, are not zero at 90 deg inclination, as suggested by some models.

Figure 8 shows the effect of varying the ''exposure ratio'' (R_{exp}), which is the ratio of aperture diameter to cavity diameter. Overall convection loss is obviously higher for a larger exposure ratio (ie larger aperture for the same sized cavity). The inclination for which maximum convection loss occurs increases as the exposure ratio decreases, which was also observed by Leibfried [8].

4.2 Synthetic Schlieren Images and Numerical Results Schlieren images of the 0 deg angle are shown in Fig. 9. For reference, a schematic outline of the cavity cross section at the mid plane is superimposed on these images with the dotted line representing the cavity and a dash marking the center of the aperture.

Figure 9(*a*) is an instantaneous image while Fig. 9(*b*) is an average image over one minute. The comparison shows that the plume is steady as it leaves the cavity and becomes unstable above the model receiver. It is important to note that the flow is three dimensional and the schlieren images only provide qualitative images of the flow pattern.

Figure 10 shows instantaneous Schlieren, numerical temperature and velocity profiles of the symmetric plane of the model at receiver angles of 0 deg, 30 deg and 60 deg. The Schlieren images show regions of highest temperature gradient as the brightest. Comparison with the numerically calculated temperature distributions shows good qualitative agreement. It should be noted though, that the CFD calculation is predicting the time average distribution rather than instantaneous. It can be seen from the 0

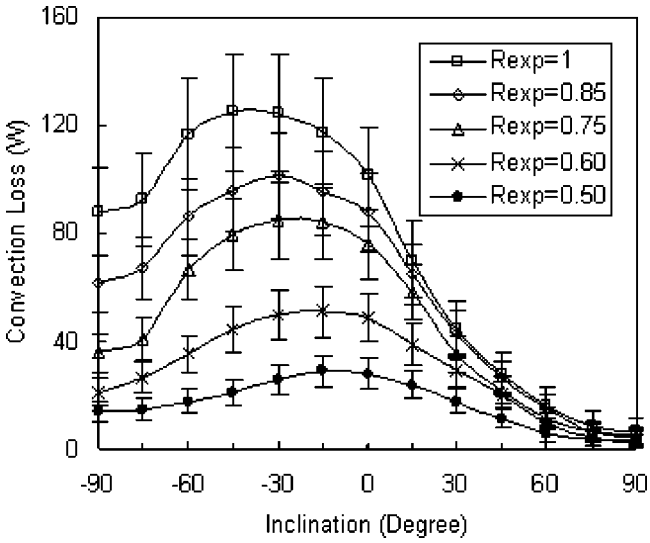

Fig. 8 Convection heat loss for various exposure ratios with Tc=445 deg C

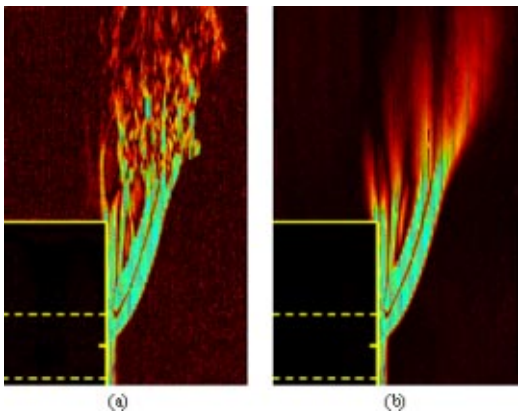

Fig. 9 Schlieren images at a receiver angle of 0 deg, with Tc =445 deg C and fully open cavity: (*a*) instantaneous (*b*) average

and 30 deg schlieren images that flow becomes turbulent above the front edge of the model while with the 60 deg angle it is relatively steady.

The similarity between temperature and velocity profiles of Fig. 10(*d*)–(*i*) indicates the strong coupling between momentum and energy in natural convection. In each figure the color represents the relative magnitude and so cannot compare to those in other figures. It is evident that the predicted flow pattern is in agreement with what is intuitively expected. At an angle of 0 deg, the cold air enters the cavity at the lower half of the aperture and flows along the lower part of the cavity where it is heated. The air reaches the back wall and flows upward until it encounters the upper cavity wall. The air then flows back along it and finally exits the cavity. A relatively stagnant core is observed in the middle of the cavity. The hot plume of air coming out from the upper half of the aperture flows directly upward without attachment to the frontal part of the receiver. The plume spreads out with decreasing velocity due to both the viscous effect and reduction of induced buoyancy force caused by cooling of the plume. The flow patterns when tilted at angles of 30 deg and 60 deg are quite similar but with the addition of a stagnant zone and local circulation in the upper part of the tilted cavity due to the stable stratification of temperature.

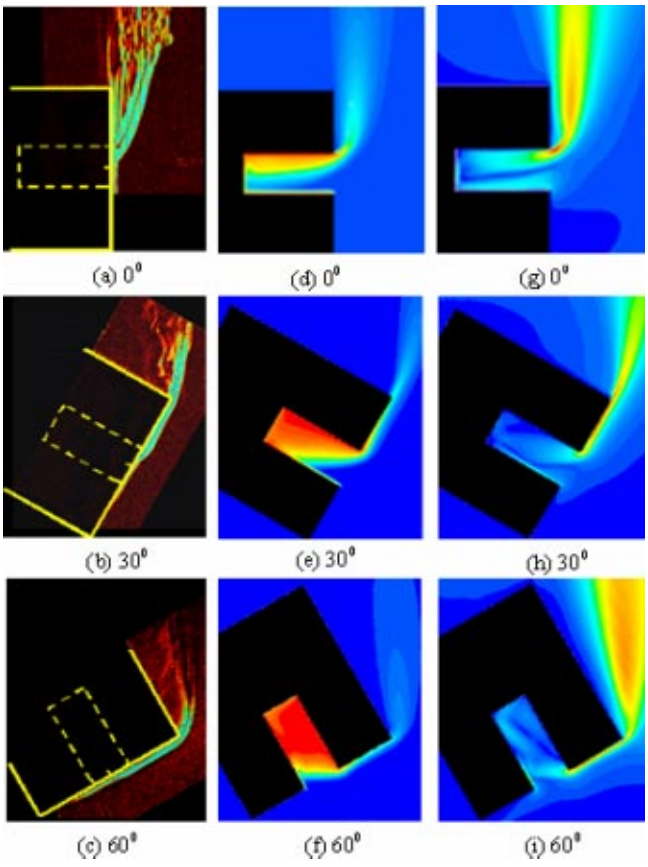

Fig. 10 Flow images for Tc=445 deg C and fully open cavity: (*a*)-(*c*) Schlieren images, (*d*)-(*f*) numerical temperature contour plots, (*g*)-(*i*) numerical velocity contour plots

Figure 11(*a*)–(*f*) shows a close up of the aperture region presented in Fig. 10(*a*)–(*f*). These images show the fraction of the aperture that the outflow occupies, which can be compared with the numerical aperture normal velocity profiles of Figs. 11(*g*)–(*i*). The outflow area represented by the area above the line of zero velocity is in good agreement with the Schlieren images and numerical temperature profiles of Figs. 11(*a*)–(*f*). With 0 deg and 30 deg the outflow occupies less than half of the aperture while with 60 deg the outflow area increases to about half the aperture, which is primarily caused by the augmentation of the stagnation zone inside the cavity.

4.3 Comparison Between Previous Studies, Numerical and Experimental Results. The experimentally measured convective heat loss for positive angles is plotted in Fig. 12 together with the results from the CFD calculations and the values calculated from correlations presented by the various authors discussed in section 1.1.

It is apparent that the CFD calculation is in good agreement at 0 and 90 deg inclinations while it overestimates at intermediate angles. The use of the Spalart-Allmaras turbulent viscosity model could be one reason for an overestimation, since the Rayleigh numbers encountered are less than 10^7, whereas several authors suggest that the transition to turbulent flow occurs as high as 10^9. It should be noted that although the cavity wall boundary condition was simplified to a constant temperature, the actual temperature distribution was also modeled for 0 deg inclination and the difference between the models is 0.2%.

Although all the correlations plotted together with the results of the present investigation show qualitatively the same dependence of heat loss on angle, there is a significant spread in magnitude. The Koenig & Marvin model [6] and Stine & McDonald model [7] predict the heat losses with the greatest deviation from the present results and those predicted by other models. This might be due to the fact that both were derived from the results obtained with actual receivers whose length scales were much greater than that of the model receiver. However, the Clausing model [1] shows the best agreement with the present result despite the fact that it was primarily derived for application to large central receiver systems. The Modified Clausing and Stine & McDonald models proposed by Leibfried [8] are comparable to each other and relatively close to the present results but not as close as the original Clausing one.

All of the correlations examined predict zero natural convective loss at 90 deg angle. This is physically implausible and indeed both the experimental measurements and CFD calculation from this study indicate that this is not the case.

Two correlations (Modified Stine and Modified Clausing) that span both negative and positive angles are compared with experimental results with $R_{exp}=1$ in Fig. 13 and $R_{exp}=0.75$ in Fig. 14. In both Figs. 13 and 14 the modified Stine correlation shows the correct qualitative behavior over the full range of inclination, but predicts higher losses than the experimental results. On the other hand the modified Clausing correlation in Fig. 13 shows a constant convection loss at negative angles and in Fig. 14 the convection loss is almost constant between −75 deg and −15 deg. This behavior is neither logical nor consistent with the experimental data and suggests a fundamental shortcoming in the formulation

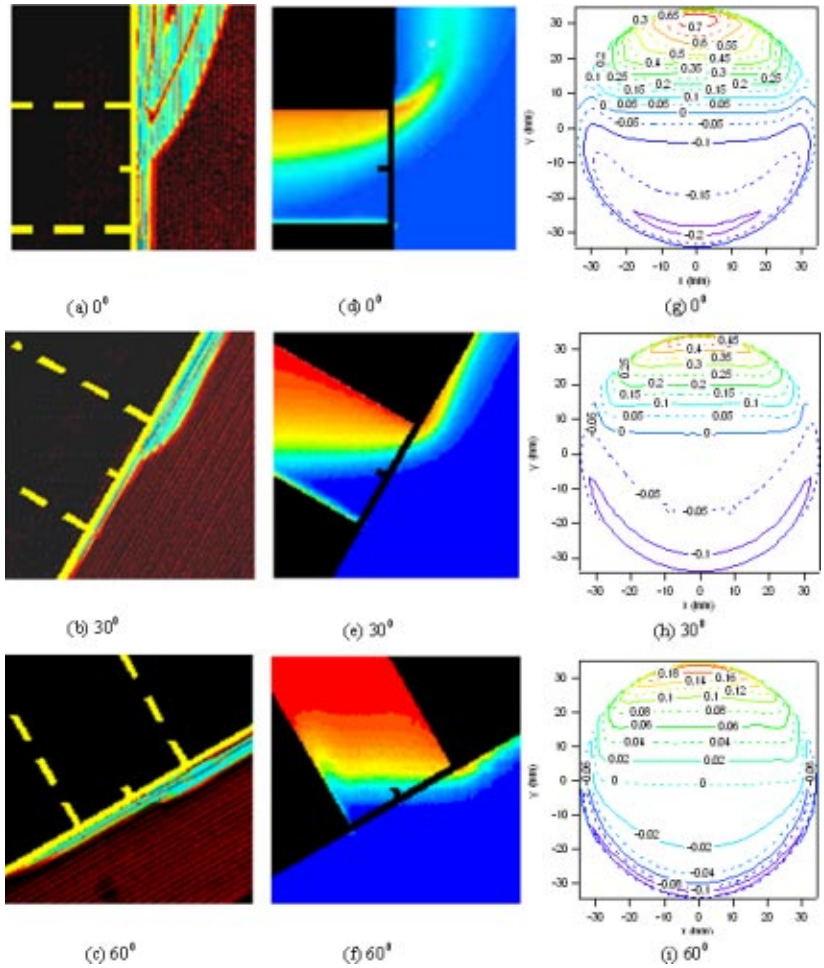

Fig. 11 Aperture region flow images for Tc=445 deg C and fully open cavity: (*a*)-(*c*) Schlieren images, (*d*)-(*f*) numerical temperature contour plots, (*g*)-(*i*) aperture normal velocity profiles

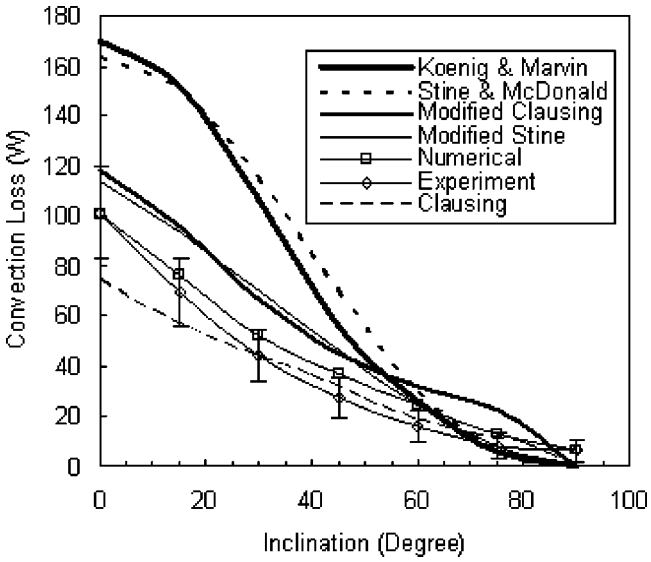

Fig. 12 Comparison of natural convection heat loss for Tc =445 deg C and fully open cavity

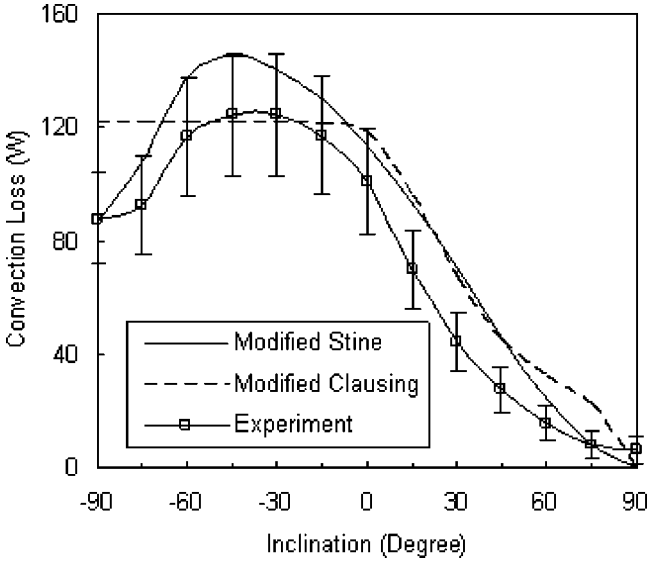

Fig. 13 Comparison of natural convection heat loss with Tc =445 deg C and fully open cavity

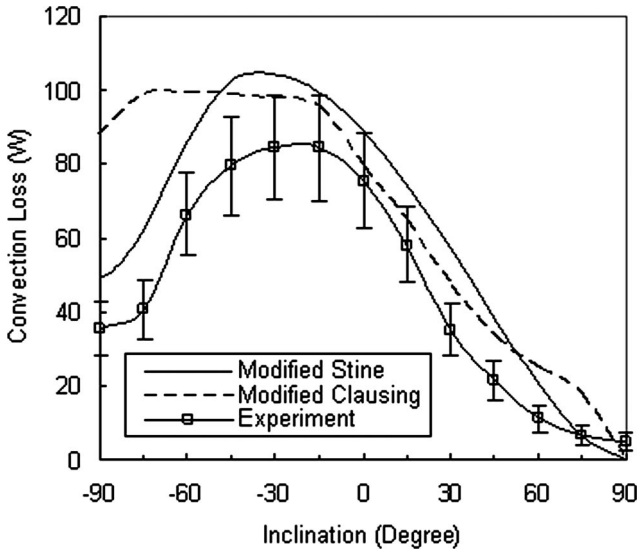

Fig. 14 Comparison of natural convection heat loss with Tc=445 deg C and Rexp=0.75

of the correlation. The main reason for this appears to be how the characteristic length is defined [8]. Part of the characteristic length is the streaming length, L_s, which is defined as the distance along the central section of the cavity wall from the lowest part of the cavity, to the beginning of the stagnant zone (where the horizontal line drawn from the upper lip of the aperture meets the cavity wall). The cavity geometry in Fig. 13 has no stagnant zone at angles between −90 deg and 0 deg and therefore L_s is constant in this region. Another variable used with this correlation is the stagnant zone area, which is the cavity wall area that lies within the stagnant zone (zone above the horizontal line drawn from the upper lip of the aperture). At negative angles, with increasing R_{exp} the variation of both L_s and A_s diminishes and hence the Modified Clausing correlation is flatter at negative angles with higher R_{exp}. As a result the Modified Clausing correlation does not appear to be suitable for the cylindrical geometry examined in this study.

5 Conclusion

The simple electrically heated simulated solar cavity receiver tested, has produced accurate repeatable direct measurements of natural convection heat loss for temperatures between 450 deg C and 650 deg C, inclination angles from 90 deg to −90 deg and aperture to cavity diameter ratios between 0.5 and 1. A good level of agreement between the measurements and CFD calculation with ''Fluent'' has been found, suggesting that predictions of losses from CFD calculations on actual solar receiver geometries can be regarded with some confidence. Comparison of the results with the predictions of a range of previously published models has shown mixed levels of agreement. The Clausing model [1] shows overall the closest prediction to both numerical and experimental results for downward facing angles despite its original use for bigger-scale central receivers. For upward facing angles the Modified Stine correlation shows the closest agreement to the experimental results. The discrepancy at an orientation of 90 deg between the present results and the predictions of all correlations taken from the literature is notable. All published models predict zero convection loss at 90 deg, which is counterintuitive and both the measurements and CFD calculations presented have shown it to be incorrect.

Experimentally, repeating the exercise for a cavity size closer to that of real receivers, would give even greater confidence on the validity of the predictions from CFD calculations. It is important to note that although operating conditions for real receivers tend to have some wind effects, it is only natural convection that is examined in this study.

Nomenclature

- A = area, m^2
- E_{bi} = black body emissive power of surface i, W/m^2
- F_{ij} = fraction of radiant energy leaving surface i and reaching surface j
- g = gravitational acceleration, m/s^2
- J_i = radiosity of surface i, W/m^2
- L = length, m
- p_L = power level
- q = heat flow rate, W
- R = resistance, Ω
- Ra = Raleigh number $= g\beta(T_w - T_\infty)L^3/\nu\alpha$
- R_{exp} = exposure ratio = aperture diameter/cavity diameter
- T = temperature, deg C, K
- V = voltage, *V*
- α = thermal diffusivity, m^2/s
- β = coefficient of thermal expansion, 1/K
- ε = emissivity
- ν = kinematic viscosity, m^2/s

Subscripts

- c = cavity
- cond = conduction
- conv = convection
- rad = radiation
- s = stagnant zone
- t = total

References

[1] Clausing, A. M., 1981, ''An Analysis of Convective Losses From Cavity Solar Central Receivers,'' Sol. Energy, **27**(4), pp. 295–300.
[2] Luzzi, A., Lovegrove, K., Paitoonsurikarn, S., Siangsukone, P., Johnston, G., Burgess, G., Joe, W., and Major, G., 2002, ''Paraboloidal Dish Solar Concentrator Investigations at the ANU-an update,'' Proc. of the International Symposium on Concentrated Solar Power and Chemical Energy Technologies, Zurich.
[3] Clausing, A. M., 1983, ''Convection Losses From Cavity Solar Receivers-Comparisons Between Analytical Predictions and Experimental Results,'' J. Sol. Energy Eng., **105**, pp. 29–33.
[4] Clausing, A. M., Waldvogel, J. M., and Lister, L. D., 1987, ''Natural Convection From Isothermal Cubical Cavities With a Variety of Side Facing Apertures,'' ASME J. Heat Transfer Trans. , **109**, pp. 407–412.
[5] Harris, J. A., and Lenz, T. G., 1985, ''Thermal Performance of Concentrator/Cavity Receiver Systems,'' Sol. Energy, **34**(2), pp. 135–142.
[6] Koenig, A. A., and Marvin, M., 1981, ''Convection Heat Loss Sensitivity in Open Cavity Solar Receivers,'' Final report, DOE contract No. EG77-C-04-3985, Department of Energy, Oak Ridge, Tennessee.
[7] Stine, W. B., and McDonald, C. G., 1989, ''Cavity Receiver Heat Loss Measurements,'' Proc. of ISES World Congress, Kobe, Japan.
[8] Leibfried, U., and Ortjohann, J., 1995, ''Convective Heat Loss From Upward and Downward-Facing Cavity Solar Receivers: Measurements and Calculations,'' J. Sol. Energy Eng., **117**, pp. 75–84.
[9] Dalziel, S. B., Hughes, G. O., and Sutherland, B. R., 2000, ''Whole-Field Density Measurements by 'Synthetic Schlieren,' '' Exp. Fluids, **28**, pp. 322–335.
[10] Dalziel, S. B., 1992, ''Decay of Rotating Turbulence: Some Particle Tracking Experiments,'' Appl. Sci. Res., **49**, pp. 217–244.
[11] Holman, J. P., 1997, *Heat Transfer*, 8th ed., McGraw-Hill, New York.
[12] McDonald, C. G., 1995, ''Heat Loss from an Open Cavity,'' Sandia National Laboratories, California.
[13] Fluent Inc., 2002, Fluent 6 User Guide.
[14] Spalart, P. R., 2000, ''Strategies for Turbulent Modeling and Simulations,'' Int. J. Heat Fluid Flow, **21**, pp. 252–263.